Iraqi Geological Journal

Journal homepage: https://www.igj-iraq.org

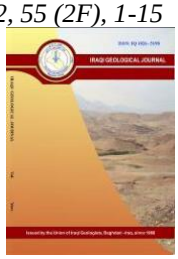

Geochemical Criteria for Discriminating Shallow and Deep Environments in Oligocene-Miocene Succession, Western Iraq

Farah H. Turki[1,*], Salih M. Awadh[1]

[1] Department of Geology, College of Science, University of Baghdad, Baghdad, Iraq

* **Correspondence**: farah.hazem1208m@sc.uobaghdad.edu.iq

Received:
17 October 2022

Accepted:
24 November 2022

Published:
31 December 2022

Abstract

The geochemical study of the Oligocene-Miocene succession Anah, Euphrates, and Fatha formations, western Iraq, was carried out to discriminate their depositional environments. Different major and trace patterns were observed between these formations. The major elements (Ca, Mg, Fe, Mn, K, and Na) and trace elements (Li, V, Cr, Co, Ni, Cu, Zn, Ga, Rb, Sr, Zr, Cs, Ba, Hf, W, Pb, Th, and U) are a function of the setting of the depositional environments. The reefal facies have lower concentrations of MgO, Li, Cr, Co, Ni, Ga, Rb, Zr, and Ba than marine and lagoonal facies but have higher concentrations of CaO, V, and Sr than it. Whereas dolomitic limestone facies are enriched V, and U while depletion in Li, Cr, Ni, Ga, Rb, Sr, Zr, Ba, and Pb Conversely, the lagoonal facies are rich in clay minerals and associated trace elements Li, V, Cr, Co, Ni, Cu, Ga, Rb, Zr, Ba, and Pb.

Keywords: Geochemical data; Depositional environments; Anah Formation; Euphrates Formation; Fatha Formation

1. Introduction

Geochemical criteria as indicators for depositional environments are a significant topic in understanding and solving the problem of defining deposited environments. Several authors, for example, Bilings and Ragland (1968) and Al-Bassam and Saeed (1980), used trace elements to discriminate between the reef and non-reef carbonate facies. The geochemical indices, degree of pyritization (DOP), C/S, U/Th, V/Cr, Ni/V, Ni/Co, authigenic uranium, and (Cu+ Mo)/Zn)) were used to interpret bottom water paleo-oxygen concentration for argillaceous sedimentary rocks (Jones and Manning, 1994). Redox-sensitive trace elements (V, Co, Ni, and Mo) are used to infer the hydrocarbon origin and the organic matter depositional conditions (Awadh and Al-Ankaz, 2016). Major elements (Al, Ca, Fe, Mg, K, P, Si, Ti) and trace elements (Ba, Pb, Rb, Sr, V, Zn, Zr) are used as evidence for a change in depositional energy conditions of tidal-flat sediments (Dellwig et al., 2000). B/K, Br/K, I/K, Na/K, S/K, Ge/K, and U/K were used for interpreting paleosalinity related to relative sea-level change (López-Buendıa et al., 1999). Geochemical proxies (CIA= chemical index of alteration, Zr/Ti, Rb/K, V/Cr, and organic carbon content) are used to explain variation in depositional conditions (Scheffler et al., 2006). Stable carbon and nitrogen isotopes and elemental composition and origin of organic matter were used by Awadh (2014) to discriminate marine and terrestrial environments.

The author's conclusions often do not agree in distinguishing the various environments, so inconsistencies may arise. This discrepancy may be due to the use of different methods or the omission of certain evidence. In this research, complete mineralogical and geochemical data have been employed

DOI: 10.46717/igj.55.2F.1ms-2022-12-16

to address this issue. This application is significantly important in interpreting different types of sedimentary environments worldwide. Currently, the research focuses on the Oligocene-Miocene succession represents a sequence of regression- transgression of sea level in the Western Desert of Iraq (Sissakian and Mohammed, 2007; Awadh and Hussien, 2015) Anah, Euphrates, and Fatha formations are a good case study to be investigated due to they having different types of known sedimentary environments. This research uses full mineralogical and geochemical data to discriminate between shallow (reef and lagoon) and deep environments.

2. Geological Setting

The study area is located in the Al-Anbar, within a Stable Shelf extending along the western side of the Euphrates River (Fig.1). Anah, Euphrates, and Fatha formations represent the stratigraphic succession. The Anah Formation of the late Oligocene age is composed of fossiliferous limestone deposited in a shallow, warm environment with low to moderate energy levels (Al-Sayyab and Al-Hamdani., 1990) reef-backreef environments. It is unconformably overlain by the Euphrates Formation, emplacement on a thick basal conglomerate (Al-Obaidy, 2015).

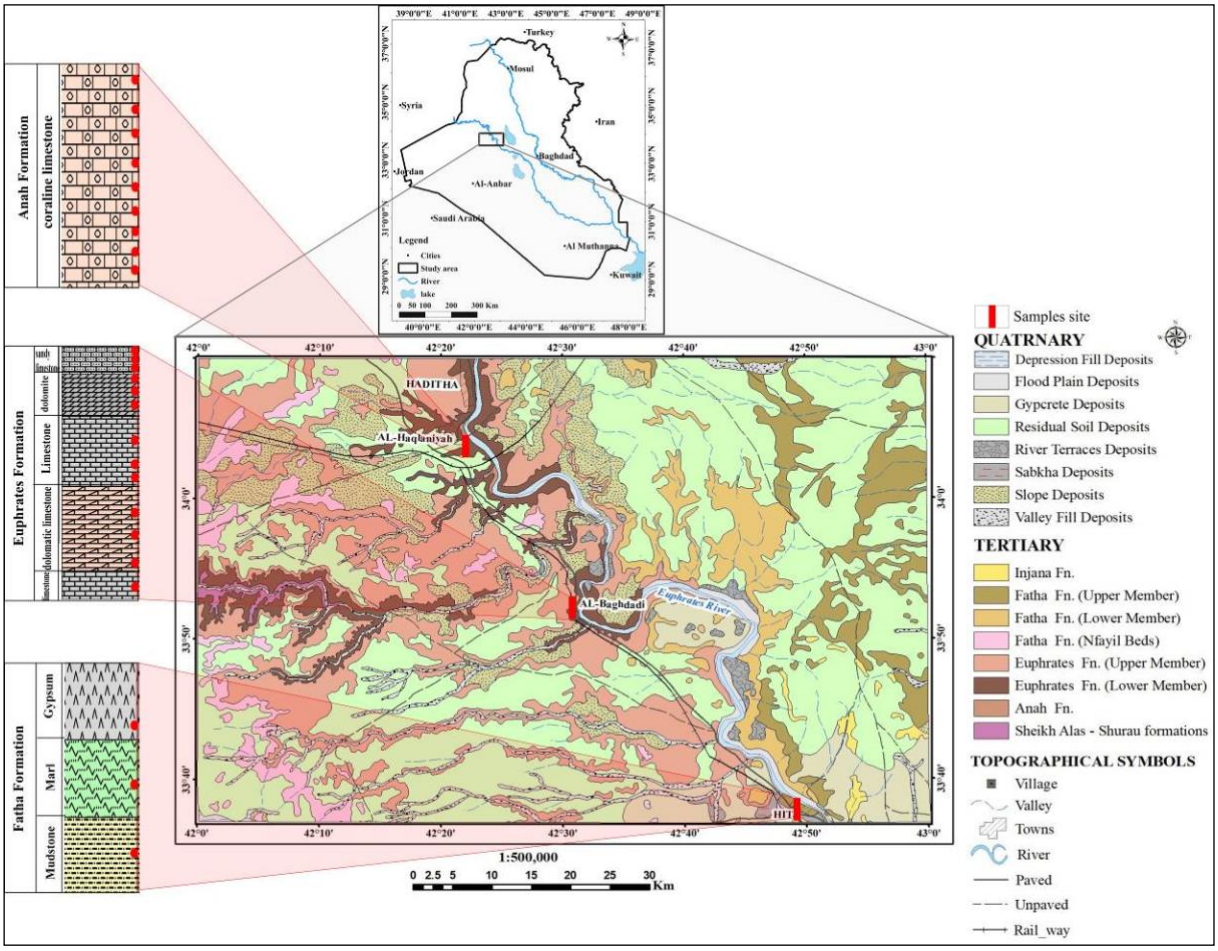

Fig.1. Geological map of the study area (GEOSURV, 2013)

The Euphrates Formation is of the Early Miocene age and composed of shelly, chalky, well-bedded recrystallized limestone (Jassim and Goff, 2006) deposited in open to restricted platforms which indicated lagoonal environment with warm and restricted open circulation (Al-Dabbas et al., 2013, and Al-Dabbas et al., 2014). The sedimentary environments of the Euphrates Formation have been divided into three environments (lagoon environment, back shelf, and open shelf) (Mohammed and

Nasser,2018). The Fatha Formation (Middle Miocene) existed as separated small hills due to weathering and erosion, it comprises anhydrite, gypsum, and salt, interbedded with limestone and marl (Jassim and Goff, 2006). All researchers agree it was deposited under a marine environment based on lithofacies characteristics and fossil content (Al-Ankaz, 2016). The Quaternary sediments cover the Euphrates Formation in most areas. The Pleistocene sediments are heterogeneous of fine pebbles consisting of quartz, chert, carbonate rock fragments, and clay (Awadh and Ahmed, 2013).

3. Materials and Methods

A total of 30 samples were collected from the Oligocene-Miocene succession, from bottom to top of outcrops which includes Anah, unconformity zone, Euphrates, and Fatha formations from Wadi Haqlan, Al-Baghdadi, and Hit in western Iraq (Table 1). Fourteen reefal carbonate samples containing skeletal organisms from the Anah Formation and unconformity zone (1AWH, 2AWH, 4AWH, 5AWH, 6AWH, 7AWH, 8AWH, 9AWH, 10AWH, 1UB, 2UB, 3UB,4UB, and 3UWH), Thirteen dolomitized limestone samples from the Euphrates Formation (5EB, 6EB, 7EB, 8EB, 9EB, 10EB,11EB, 12EB, 13EB, 14EB, 11EWH, 12EWH, and 13EWH), and three samples of gypsiferous marly limestone were collected from lower member of the Fatha Formation (1FH, 2FH, and 3FH). All those samples were crushed, sieved to <2mm, homogenized, and managed to be representative samples according to the procedure stated in Tucker (1988). X-ray diffraction (XRD) and geochemical analyses were performed. The XRD analysis was done in the Ministry of Sciences and Technology laboratory to identify the mineralogical composition of seven samples (1AWH, 1UB, 3UWH, 5EB, 9EB,14EB, and 2FH). Geochemical analyses for major oxides (SiO_2, Al_2O_3, Fe_2O_3, TiO_2, CaO, MgO, MnO, Na_2O, K_2O, and P_2O_5) and trace elements (Li, V, Cr, Co, Ni, Cu, Zn, Ga, Rb, Sr, Zr, Cs, Ba, Hf, W, Pb, Th, and U) were analyzed by inductively coupled plasma-mass spectrometry (ICP-MS) at the Analytical Chemistry and Testing Services, Mineral Division-ALS Chemex at Sevilla, Spain for seventeen samples (1AWH, 9AWH, 10AWH, 2UB, 4UB, 3UWH, 5EB, 7EB, 8EB, 9EB, 11EB, 12EB, 14EB, 13EWH, 1FH, 2FH, and 3FH). The reliability of the analytical results was accurate.

Table 1. The coordinates of the study area

Area	Easting	Northing
Wadi Haqlan	42˚ 22′ 01.00″	34˚ 05′ 25.50″
Al-Baghdadi	42˚ 31′ 48.60″	33˚ 51′ 36.35″
Hit	42˚ 48′ 41.05″	33˚ 38′ 13.93″

4. Results and Discussion

4.1. Mineralogy

Seven samples were mineralogically analyzed using XRD. The results of XRD are listed in Table 2. The pure calcite in the Anah Formation pointed out reef facies unaffected by dolomitization (Fig. 2 a). Calcite is the predominant mineral in the unconformity zone in the study area (Fig. 2 b and c). The Euphrates Formation consists of calcite (Fig. 2 d), dolomite, a rare amount of gypsum (Fig. 2 e), chlorite, and illite (Fig.3 b). Dolomite, quartz and, clay minerals characterize the Fatha Formation (Fig. 3 c and d). The Anah Formation designated by coral facies was not affected by the dolomitization process. This indicates that the sedimentary basin during the Oligocene period was uplifted, forming a shallow barrier reef. Then the basin slightly subsided, and carbonates were deposited in a shallow marine to the open sea environment forming the Euphrates Formation. The diagenetic process of dolomitization was dominant due to the availability of Mg-rich solutions (Tucker et al., 2009). This can be noted in Fig.4

as MgO increased when CaO decreased. The basin becomes shallow depositing Fatha Formation in a lagoonal environment with high salinity, and the clay minerals indicate a continental supplement.

Table 2. XRD data display the 2- thetas and d-space of each mineral

Sample No.	Minerals	2theta	d-spacing	Sample No.	Minerals	2theta	d-spacing
1AWH	Calcite	23.377	3.802	9EB	Calcite	23.413	3.796
		29.717	3.000			29.762	2.999
		36.283	2.473			36.331	2.470
		39.719	2.267			39.772	2.264
		43.472	2.079			43.520	2.077
		47.448	1.914			47.493	1.912
		47.814	1.900			47.867	1.898
		48.814	1.864			48.869	1.862
1UB	Calcite	23.368	3.803	14EB	Dolomite	24.279	3.662
		29.714	3.004			31.147	2.869
		36.280	2.474			33.732	2.654
		39.715	2.267			35.503	2.526
		43.476	2.079			37.567	2.392
		47.441	1.914			41.326	2.182
		47.820	1.900			44.014	2.055
		48.824	1.863			45.135	2.007
						49.458	1.841
3UWH	Calcite	23.411	3.796		Calcite	29.700	3.008
		29.751	3.000				
		36.322	2.471				
		39.755	2.265				
		43.507	2.078				
		47.476	1.913				
		47.838	1.899				
		48.856	1.862				
5EB	Calcite	23.418	3.795	2FH	Dolomite	24.190	3.676
		29.762	2.999			31.026	2.880
		36.330	2.470			33.564	2.667
		39.772	2.264			35.404	2.533
		43.519	2.077			37.467	2.398
		47.488	1.913			41.208	2.188
		47.865	1.898			43.913	2.060
		48.879	1.861			45.022	2.011
	Dolomite	31.755	2.818			49.318	1.846
					Quartz	21.078	4.211
						26.843	3.318
	Gypsum	11.850	7.469		Palygorskite	8.691	10.165
					Chlorite	12.350	7.167
					Illite	8.700	10.164
					Vermiculite	6.050	14.610

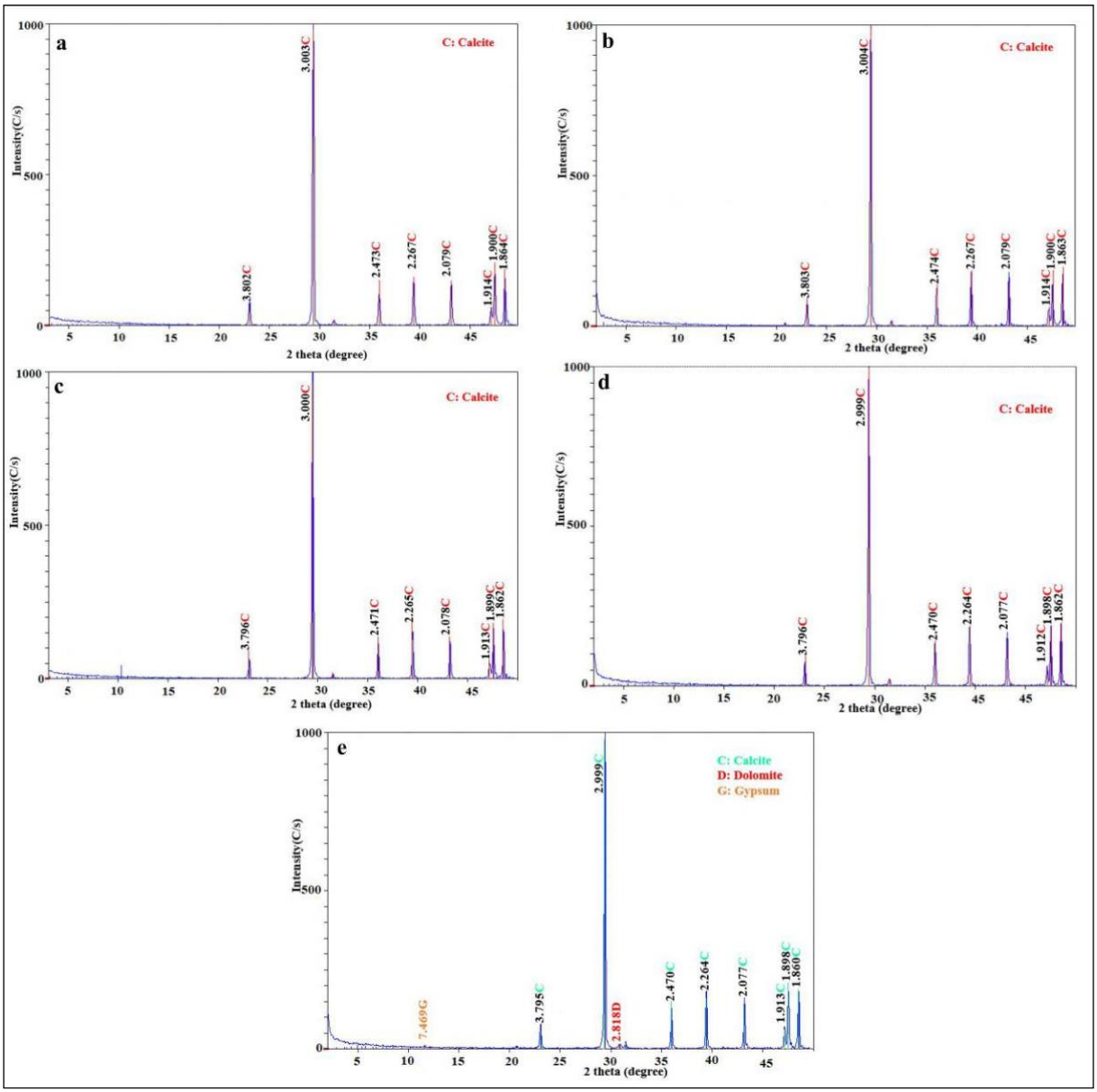

Fig.2. X-ray diffractograms show the peak reflections of the minerals in Anah, unconformity, and Euphrates formations, sample no.1AWH (a); 1UB (b); 3UWH (c); 9EB (d) show calcite reflections, and sample no. 5EB (e) shows calcite, dolomite, and gypsum reflections.

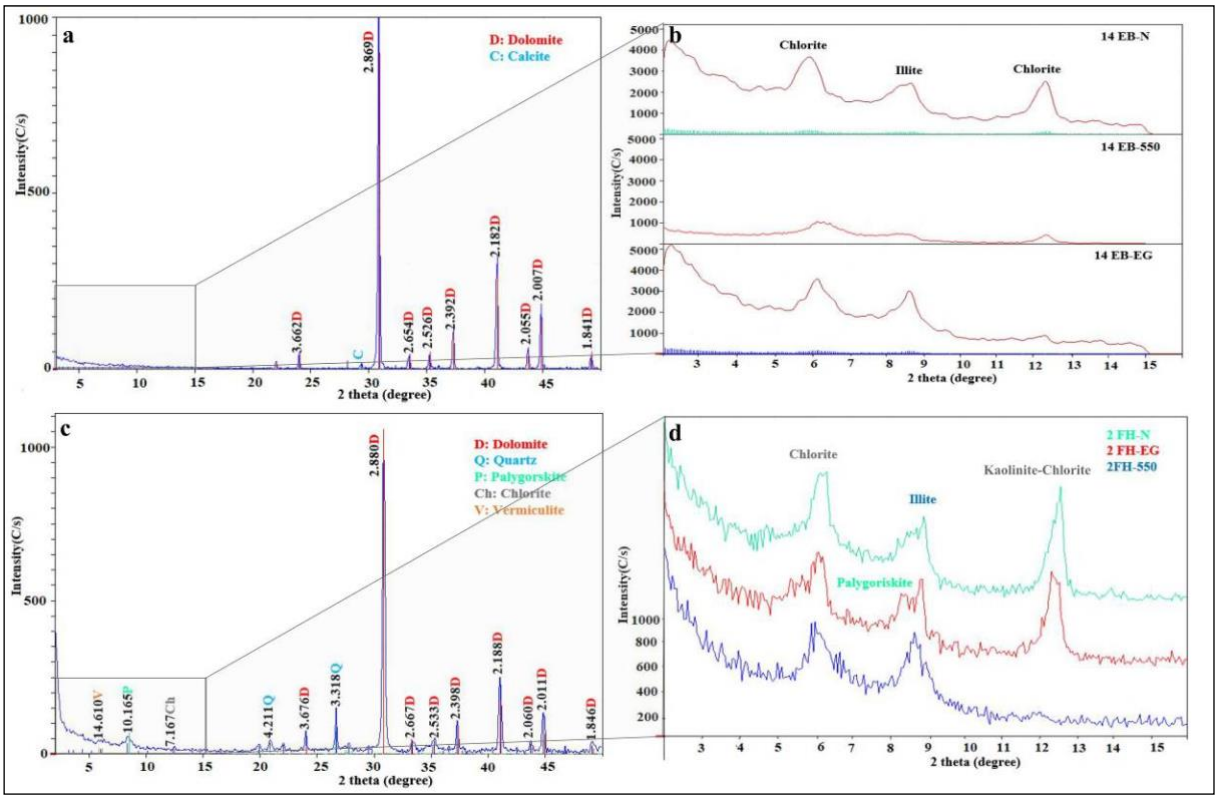

Fig.3. X-ray diffractograms show the peak reflections of the minerals in the Euphrates and Fatha formations, sample no. 14EB shows calcite and dolomite (a), chlorite and illite (b); sample no. 2FH shows dolomite, quartz, palygorskite, vermiculate, chlorite and illite (c and d).

4.2. Geochemistry

Seventeen samples of carbonates were selected from the Oligocene-Miocene succession Anah, Unconformity zone, Euphrates, and Fatha formations. The results of samples analyzed for major oxides (SiO_2, Al_2O_3, Fe_2O_3, CaO, MgO, Na_2O, K_2O, TiO_2, MnO, and P_2O_5) and trace elements (Li, V, Cr, Co, Ni, Cu, Zn, Ga, Rb, Sr, Zr, Cs, Ba, Hf, W, Pb, Th, and U) are listed in Tables 3 and 4 respectively. They are normalized to the Post Archean Australian Shale (PAAS) based on (Taylor and McLennan,1985).

The major oxides (SiO_2, Al_2O_3, Fe_2O3, MgO, Na_2O, K_2O, MnO, TiO_2, and P_2O_5) increase upward from Anah < Unconformity < Euphrates < Fatha formations, whereas CaO decreased upward (Fig. 4). These results are consistent with mineralogical phases. The Anah Formation has a wide range (%) of CaO from 55.6 to 56.1 compared to other formations in the study area due to the predominance of calcite. The content of MgO (0.34-0.47%) is significantly less than others, reflecting no dolomitization. LOI in Anah Formation ranged from 43.4% to 43.7%, originating from calcite. The unconformity zone shows a slight decrease in the content of CaO (31-55.3 %), reflecting high carbonate variation. High variation of dolomitization related to magnesia content varies from 0.52% to18.7%. Dolomite and calcite participated with a high value of LOI (43.5-45.1%). The relative decrease in CaO in the Euphrates Formation (31.9-55%) was reported with dolomitization as MgO ranged from 0.63% to 20.1%. On the other hand, the Fatha Formation has a relatively narrow range of CaO (10.9-33.3%) due to the dominance of the clay minerals and marl. Clay minerals and marl participated with some of the MgO that ranges from 0.46 to 15.70%. The LOI of the lower part of the Fatha Formation ranges from 21.5 to 36.8%, indicating clay minerals, marl, and gypsum.

Table 3. Major oxides (%), statistical calculated, and average PAAS of the formations studied

S. No.		SiO_2	Al_2O_3	Fe_2O_3	CaO	MgO	Na_2O	K_2O	TiO_2	MnO	P_2O_5	LOI	Total
							%						
1AWH	Anah Formation	0.17	0.07	0.05	56.1	0.340	0.04	0.009	0.009	0.010	0.009	43.7	100.52
9AWH		0.35	0.10	0.06	55.7	0.470	0.03	0.010	0.010	0.010	0.020	43.4	100.19
10AWH		0.36	0.13	0.11	55.6	0.390	0.04	0.009	0.010	0.009	0.009	43.6	100.29
Min		0.17	0.07	0.05	55.6	0.340	0.03	0.009	0.009	0.009	0.009	43.4	100.19
Max		0.36	0.13	0.11	56.1	0.470	0.04	0.010	0.010	0.010	0.020	43.7	100.52
Ave.		0.29	0.10	0.07	55.8	0.400	0.04	0.009	0.009	0.009	0.012	43.5	100.30
St. Dev.		0.08	0.02	0.02	0.21	0.050	0.004	0.0004	0.0004	0.0004	0.005	0.12	0.1300
2UB	Unconformity	2.76	0.70	0.60	31.0	18.70	0.14	0.200	0.040	0.010	0.020	45.1	99.290
4UB		0.67	0.11	0.12	55.3	0.650	0.03	0.010	0.010	0.009	0.010	43.5	100.44
3UWH		0.22	0.09	0.08	55.2	0.520	0.03	0.010	0.010	0.010	0.009	43.6	99.790
Min		0.22	0.09	0.08	31.0	0.520	0.03	0.010	0.010	0.009	0.009	43.5	99.290
Max		2.76	0.70	0.60	55.3	18.70	0.14	0.200	0.040	0.010	0.020	45.1	100.44
Ave.		1.21	0.30	0.26	47.1	6.620	0.06	0.070	0.020	0.009	0.013	44.0	99.840
St. Dev.		1.10	0.28	0.23	11.4	8.530	0.05	0.080	0.010	0.0004	0.004	0.73	0.4700
5EB	Euphrates Formation	0.75	0.17	0.12	54.5	0.630	0.11	0.040	0.010	0.010	0.009	43.3	99.670
7EB		0.88	0.24	0.18	32.6	18.95	0.20	0.070	0.010	0.010	0.010	46.5	99.670
8EB		0.89	0.20	0.15	32.3	19.45	0.13	0.060	0.010	0.010	0.030	46.5	99.750
9EB		0.38	0.10	0.08	55.0	0.640	0.03	0.020	0.010	0.009	0.010	43.6	99.900
11EB		0.51	0.15	0.08	53.8	1.380	0.07	0.030	0.010	0.009	0.020	43.6	99.680
12EB		0.87	0.22	0.19	32.0	19.60	0.13	0.060	0.010	0.010	0.040	46.4	99.550
14EB		0.52	0.13	0.12	31.9	20.10	0.10	0.030	0.010	0.010	0.080	46.8	99.820
13EWH		0.42	0.10	0.15	51.2	2.630	0.75	0.210	0.010	0.009	0.020	43.6	99.110
Min		0.38	0.10	0.08	31.9	0.630	0.03	0.020	0.010	0.009	0.009	43.3	99.110
Max		0.89	0.24	0.19	55.0	20.10	0.75	0.210	0.010	0.010	0.080	46.8	99.900
Ave.		0.65	0.16	0.13	42.9	10.42	0.19	0.060	0.010	0.009	0.027	45.0	99.640
St. Dev.		0.20	0.04	0.04	10.7	9.120	0.21	0.050	0.000	0.0004	0.022	1.51	0.2200
1FH	Fatha Formation	37.2	8.66	5.19	10.9	11.15	0.60	2.030	0.500	0.070	0.120	22.7	99.200
2FH		15.9	3.40	2.00	23.9	15.7	0.30	0.840	0.200	0.050	0.060	36.8	99.220
3FH		0.60	0.13	0.06	33.3	0.46	0.03	0.05	0.01	0.009	0.01	21.5	99.420
Min		0.60	0.13	0.06	10.9	0.46	0.03	0.05	0.01	0.009	0.01	21.5	99.2
Max		37.2	8.66	5.19	33.3	15.7	0.6	2.03	0.5	0.07	0.12	36.8	99.42
Ave.		17.9	4.06	2.4	22.7	9.10	0.31	0.97	0.23	0.04	0.063	27	99.28
St. Dev.		15	3.5	2.1	9.1	6.3	0.23	0.81	0.20	0.02	0.04	6.94	0.099
PAAS*		62.8	18.9	7.22	1.30	2.20	1.20	3.700	1.00	0.11	0.16	6.00	104.59

*PAAS; Post Archaean Australian Shales (Taylor and McLennan, 1985)

Table 4. Trace elements (ppm) content and average values PAAS and GSCR of the formations studied

S. No.		Li	V	Cr	Co	Ni	Cu	Zn	Ga	Rb	Sr	Zr	Cs	Ba	Hf	W	Pb	Th	U
		Ppm																	
1AWH	Anah Formation	9.90	4.90	10.0	0.90	1.00	31.4	151	0.20	0.60	110.5	3.00	0.06	4.00	0.10	0.90	12.0	0.04	0.37
9AWH		9.90	19.0	9.90	2.00	0.90	26.0	13.0	0.30	0.90	229.0	2.00	0.08	3.20	0.09	1.00	1.90	0.11	5.54
10AWH		9.90	5.00	10.0	2.00	3.00	10.0	50.0	0.50	0.60	190.0	4.00	0.24	8.30	0.10	1.00	9.00	0.10	0.23
Min		9.90	4.90	9.90	0.90	0.90	10.0	13.0	0.20	0.60	110.5	2.00	0.06	3.20	0.09	0.90	1.90	0.04	0.23
Max		9.90	19.0	10.0	2.00	3.00	31.4	151	0.50	0.90	229.0	4.00	0.24	8.30	0.10	1.00	12.0	0.11	5.54
Ave.		9.90	9.63	9.96	1.63	1.63	22.4	71.3	0.33	0.70	176.5	3.00	0.13	5.16	0.09	0.96	7.63	0.08	2.04
St. Dev.		0.00	6.62	0.04	0.51	0.96	9.08	58.3	0.12	0.14	49.31	0.81	0.08	2.23	0.004	0.04	4.23	0.03	2.47
2UB	Unconformity	20.0	34.0	20.0	3.00	11.0	50.0	239	1.30	10.1	99.70	14.0	1.19	40.0	0.30	1.00	16.0	0.63	1.02
4UB		9.90	11.0	20.0	2.00	0.90	20.0	106	0.30	1.70	130.5	5.00	0.19	78.7	0.10	1.00	9.00	0.38	2.65
3UWH		9.90	12.0	10.0	0.90	2.00	10.0	56.0	0.50	0.70	129.0	2.00	0.07	2.60	0.10	0.90	8.00	0.07	0.38
Min		9.90	11.0	10.0	0.90	0.90	10.0	56.0	0.30	0.70	99.70	2.00	0.07	2.60	0.10	0.90	8.00	0.07	0.38
Max		20.0	34.0	20.0	3.00	11.0	50.0	239	1.30	10.1	130.5	14.0	1.19	78.7	0.30	1.00	16.0	0.63	2.65
Ave.		13.2	19.0	16.6	1.96	4.63	26.6	134	0.70	4.16	119.7	7.00	0.48	40.4	0.16	0.96	11.0	0.36	1.35
St. Dev.		4.80	10.6	4.71	0.85	4.52	16.9	77.2	0.43	4.21	14.17	5.09	0.50	31.06	0.09	0.04	3.55	0.22	0.95
5EB	Euphrates Formation	9.90	13.0	10.0	2.00	0.90	2.70	15.0	0.50	2.10	252.0	10.0	0.16	8.30	0.20	0.90	6.00	0.25	3.55
7EB		10.0	22.0	10.0	2.00	3.00	2.80	15.0	0.70	2.50	97.30	5.00	0.19	11.4	0.10	1.00	1.90	0.24	4.07
8EB		10.0	35.0	9.90	2.00	1.00	9.00	46.0	0.60	1.90	101.0	6.00	0.16	5.80	0.10	1.00	6.00	0.19	12.0
9EB		9.90	8.00	9.90	1.00	0.90	11.0	6.00	0.30	0.80	217.0	2.00	0.06	2.70	0.09	0.90	3.00	0.22	2.94
11EB		9.90	5.00	9.90	1.00	0.90	12.7	67.0	0.40	2.00	195.0	7.00	0.08	2.40	0.20	1.00	6.00	0.08	2.01
12EB		10.0	14.0	10.0	1.00	5.00	32.6	149	0.70	2.40	95.00	5.00	0.16	6.40	0.10	1.00	10.0	0.14	3.51
14EB		10.0	7.00	9.90	0.90	3.00	13.0	69.0	0.40	1.00	108.5	3.00	0.09	5.20	0.09	0.90	7.00	0.14	2.12
13EWH		9.90	14.0	10.0	2.00	0.90	14.6	64.0	0.20	1.30	146.0	5.00	0.18	5.20	0.10	0.90	7.00	0.11	5.28
Min		9.90	5.00	9.90	0.90	0.90	2.70	6.00	0.20	0.80	95.00	2.00	0.06	2.40	0.09	0.90	1.90	0.08	2.01
Max		10.0	35.0	10.0	2.00	5.00	32.6	149	0.70	2.50	252.0	10.0	0.19	11.4	0.20	1.00	10.0	0.25	12.0
Ave.		9.95	14.8	9.95	1.48	1.95	12.3	53.8	0.48	1.75	151.4	5.37	0.14	5.92	0.12	0.95	5.86	0.17	4.43
St. Dev.		0.05	9.13	0.05	0.51	1.45	8.75	43.1	0.17	0.59	57.90	2.28	0.04	2.73	0.04	0.05	2.33	0.05	3.02
1FH	Fatha Formation	50.0	111	420	23.0	273	44.0	71.0	10.4	57.9	115.5	105	2.76	123	2.60	2.00	34.0	4.13	2.65
2FH		30.0	52.0	260	9.00	79.0	50.0	54.0	4.40	20.3	196.0	58.0	1.68	55.1	1.50	1.00	20.0	1.70	2.50
3FH		9.90	7.00	9.90	0.90	1.00	1.00	3.00	0.40	1.20	411.0	2.00	0.13	16.5	0.10	1.00	1.90	0.09	0.20
Min		9.90	7.00	9.90	0.90	1.00	1.00	3.00	0.40	1.20	115.5	2.00	0.13	16.5	0.10	1.00	1.90	0.09	0.20
Max		50.0	111	420	23.0	273	50.0	71.0	10.4	57.9	411.0	105	2.76	123	2.60	2.00	34.0	4.13	2.65
Ave.		29.9	56.7	229.9	10.9	117.6	31.6	42.7	5.06	26.5	240.0	55.0	1.52	64.8	1.40	1.33	18.6	1.97	1.78
St. Dev.		16.3	42.5	168.7	9.12	114.3	21.8	28.8	4.11	23.5	124.0	42.1	1.07	44.02	1.02	0.47	13.1	1.66	1.12
PAAS*			150		23	55	50	85	20	160	200	210	15	650	5	2.7	20	14.6	3.1
GSCR**			20	11	0.1	20	4			3	610	19	0.1	10	0.3	0.6	9	1.7	2.2

*PAAS; Post Archaean Australian Shales (Taylor and McLennan, 1985)

**GSCR; Global Standard of carbonate rocks (Turekian and Wedepohl, 1961)

Table 3 presents a narrow range (%) of SiO_2 (0.17-0.36), Al_2O_3 (0.07-0.13), Fe_2O_3 (0.05-0.11), and K_2O (0.009- 0.01) in Anah Formation, which means no supply of detrital sediment, particularly quartz during deposition. The unconformity zone has SiO_2 (0.22-2.76%), Al_2O_3 (0.09-0.7%), Fe_2O_3 (0.08-0.6%), and K_2O (0.01-0.2%) slight increase observed in sample 2UB near the lower part of the section (Fig. 4). They decrease toward the overlying the Euphrates Formation, having % SiO_2 (0.38-0.89), Al_2O_3 (0.10-0.24), Fe_2O_3 (0.08-0.19), and K_2O (0.02-0.21). They increase again upwards where the Fatha Formation has % SiO_2 (0.60-37.2), Al_2O_3 (0.13 -8.66), Fe_2O_3 (0.06-5.19), and K_2O (0.05-2.03). This may explain the detrital supplement rate due to shoreline instability. The Anah Formation has Na_2O (0.03- 0.04%), TiO_2 (0.009-0.01%), MnO (0.009-0.01%), and P_2O_5 (0.009-0.02%). The average Na_2O content is 0.035% due to the low salinity of host Na and depositional solutions. Sodium ions, considered paleosalinity indicators, are one of the major dissolved constituents in seawater and diagenetic solutions (Veizer et al., 1977). The content of TiO_2 has an average of 0.009%, reflecting diminished detrital sediment. The average MnO (0.009%) is due to the low content of clay minerals because Mn has been leached from it (Till, 1971). P_2O_5 averages (0.012%) are related to the ratio of terrigenous supply during the depositional period (Al-Obaidy, 2015). The unconformity zone has a range (%) of Na_2O (0.03-0.14) and TiO_2 content has an average of 0.02% due to detrital poverty sediment. The content of MnO ranged from 0.009 to 0.01% which may be attributed to deposition positions in shallow reefal environments. P_2O_5 content has an average of 0.013%, indicating shallow environments. In the Euphrates, Na_2O (0.03-0.75%) shows a gradual increase in the exchanged ions and incorporation into lattice sites during crystallization (Fritz and Katz, 1972). The content of TiO_2 in the Euphrates (0.01%) is scarce due to a lack of clay minerals. The P_2O_5 (0.009- 0.08%) and the range of MnO (0.009- 0.01%) reflect the low rate of detrital sediment. The Fatha Formation enriched in Na_2O (0.3-0.6%) relates to the occurrence of Na as minor NaCl salt. In marine and hypersaline carbonates, the possibility of solid or liquid inclusion of NaCl has been suggested as a minor mode of Na presence in these samples (Fritz and Katz, 1972) and indicates presence mainly in clay minerals. The range of TiO_2 from 0.2 to 0.5% results from a plentiful abundance of the clay fraction. The MnO range in Fatha samples is from 0.009 to 0.07% incorporated in the clay minerals (Till, 1971). The content of P_2O_5 (0.01- 0.12%) due to the association of phosphorus with clay minerals interpreted as the presence of phosphorus in rock fragments of phosphate deposits transported from phosphatic exposure to the depositional site of Fatha Formation (Al-Obaidy, 2015). A minor element may be helpful as a geochemical indicator if there is a sizable variation in its content over a deposition basin and if this variation can be linked to a particular type of environment (Chester, 1965). Trace elements show variation behavior between Anah, unconformity, Euphrates, and Fatha formations (Fig.6). For comparison with data from the global standard average of carbonate rock (GSCR) of Turekian and Wedepohl, (1961) to reveal how the depth of sedimentary basin effected on the redistribution of trace elements. In shallow facies of Anah show depleted Ba, Cr, Hf, U, Rb, Sr, Th, U, V, Zr, Ni, and Pb relative to a standard, while Cs, W, Co, and Cu are enriched (Fig.5). Unconformity zone is enriched in Ba, Cr, Cs, Rb, W, Co, Cu, and Pb compared with standard and Hf, Sr, Th, U, V, Zr, and Ni are depleted. In contrast, Euphrates is enriched in Cs, U, W, Co, and Cu compared with standard whereas is depleted in Ba, Cr, Hf, Rb, Sr, Th, V, Zr, Ni, and Pb. Fatha samples are enriched in Ba, Cr, Cs, Hf, Rb, Th, V, W, Zr, Co, Cu, Ni, and Pb while are depleted in Sr, and U.

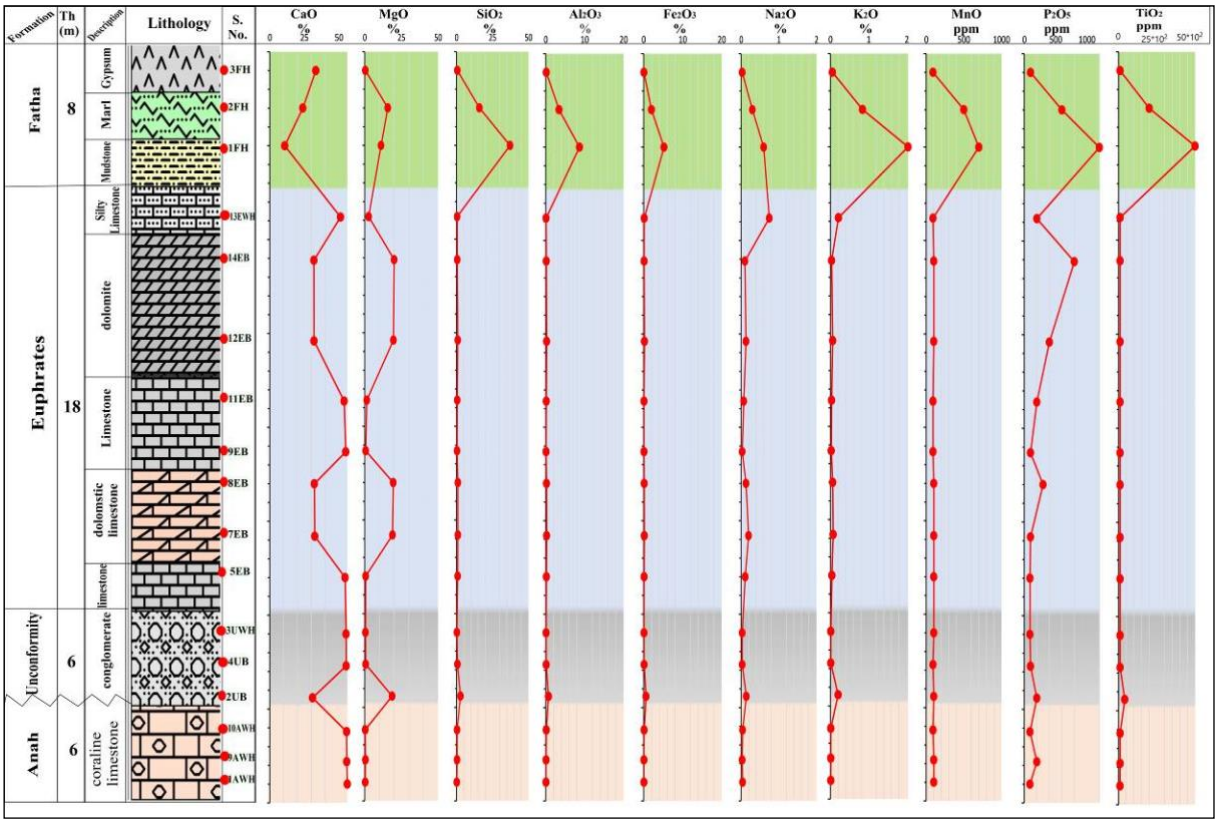

Fig. 4. Chemostratigraphic of major oxides of the different formations in the study area

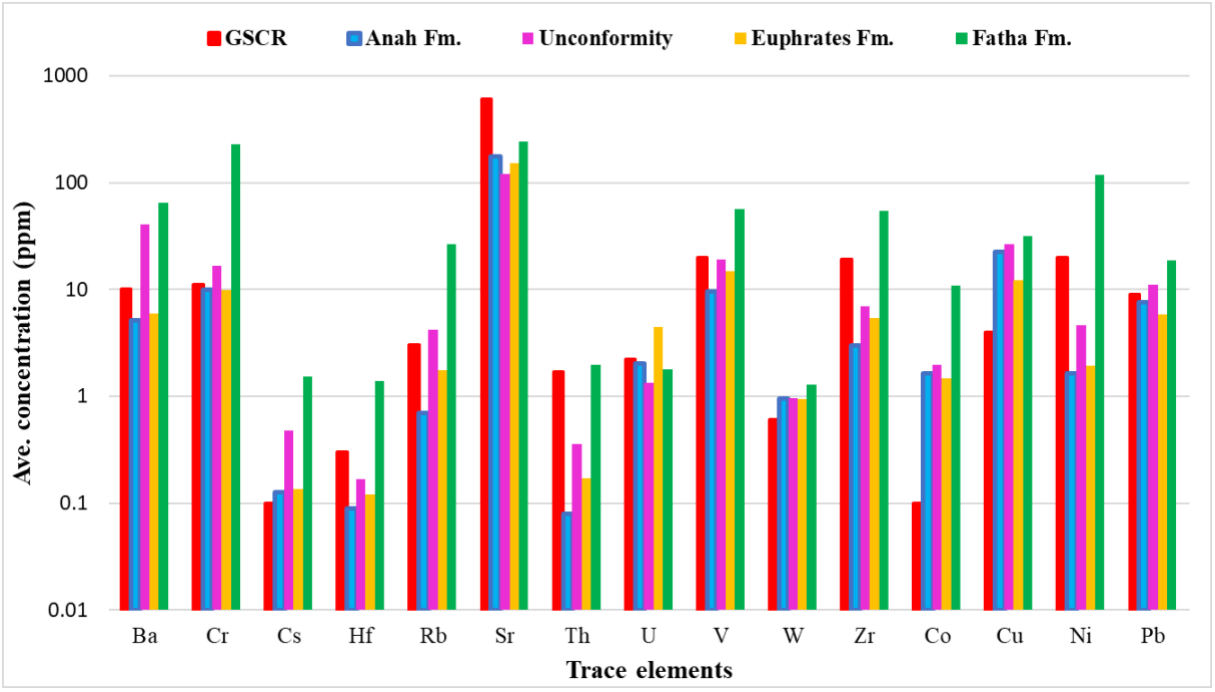

Fig.5. Trace elements contents in each formation compared with the global standard (GSCR) of Turekian and Wedepohl, 1961

Lithium (Li) concentration in the Anah is 9.9 ppm, in the unconformity zone (9.9- 20 ppm), in the Euphrates Formation (9.9- 10 ppm), in the Fatha Formation (9.9- 50 ppm) (Table 4). Vanadium (V) is a higher value in Fatha samples; an average of 56.7 ppm reflects the clay minerals association (Till, 1971).

It is in the Euphrates (5- 35 ppm), in the unconformity zone (11-34 ppm), and Anah (4.9- 19 ppm. Chromium (Cr) concentration range in the Anah, unconformity, Euphrates, and Fatha is 9-10 ppm, 10-20 ppm, 9.9-10 ppm, and 9.9- 420 ppm with an average of 9.97, 16.6, 9.95, and 229.9 ppm, respectively. Nickel (Ni) content in the Anah is 0.9- 3 ppm, in the unconformity zone (0.9- 11 ppm), in the Euphrates (0.9- 5 ppm), and the Fatha (1- 273 ppm). Ni and Cr are considered less available elements in carbonates because of their high stability in solutions, while they are simply adsorbed just at the reducing environment (Rankama and Sahama, 1951). The amount of Cobalt (Co) in the Anah is (0.9 ppm), in the unconformity zone (0.9-3 ppm), in the Euphrates (0.9-2 ppm), in Fatha samples have a wide range (0.9-23 ppm). Copper (Cu) concentration in the Anah (10- 31.4 ppm), in the unconformity zone (10- 50 ppm), in the Euphrates (2.7- 32 ppm), in the Fatha (1 -50 ppm) due to Cu may be incorporated with clay minerals. Gallium (Ga) is low mobility (Jensen et al., 2018). The concentration of Ga in Anah is (0.2-0.5 ppm), in the unconformity zone (0.3- 1.3 ppm), in the Euphrates (0.2- 0.7 ppm), and the Fatha (0.4-10.4 ppm). Rubidium (Rb) concentration in the Anah is (0.6- 0.9 ppm), in the unconformity zone (0.7-10.1 ppm), in the Euphrates (0.8- 2.5 ppm), in Fatha samples is a wide range (1.2- 57.9 ppm) this reflect associates with clay minerals because Rb resembles of geochemical behavior of K due to similarity in their ionic radii (Faure, 1997). Strontium (Sr) is present mainly in the carbonate fraction and is more concentrated in reef samples (Till, 1971). The concentration of Sr in the Anah (110.5-229 ppm), in the unconformity zone (99.7-130.5 ppm), in the Euphrates (95-252 ppm), in the Fatha (115.5- 411 ppm. Zinc (Zn) is a mobile ion during weathering process (Rankama and Sahama, 1951) in the Anah (13-151 ppm), in the unconformity zone (56-239 ppm), in the Euphrates (6-149 ppm), in the Fatha (3-71 ppm). Zirconium (Zr) concentration in the Anah ranged from 2 to 3 ppm, in the unconformity zone (2-14 ppm), in the Euphrates (2-10 ppm), and the Fatha samples are a wide range (2-105 ppm). Cesium (Cs) concentration in the Anah is (0.06-0.24 ppm), in the unconformity zone (0.07-1.19 ppm), in the Euphrates (0.06-0.19 ppm), and the Fatha (0.13-2.76 ppm). Barium (Ba) is a high concentration in Fatha Formation (16.5-123 ppm), in the Euphrates (2.4-11.4 ppm), in the unconformity zone (2.6-78.7 ppm), and the Anah (3.2-8.3 ppm) due to Ba is associated with various phases in marine sediments, including carbonates, organic matter, opal, ferromanganese oxyhydroxides, terrestrial, silicates and other detrital material and barite (Gonneea and Paytan, 2006). Hafnium (Hf) concentration in the Anah is ranged from 0.09 to 0.10 ppm, in the unconformity zone (0.1-0.3 ppm), in the Euphrates (0.09-0.2 ppm), in the Fatha (0.1- 2.6 ppm). Lead (Pb) concentration in the Anah is (1.9 -12 ppm), in the unconformity zone (8-16 ppm), in the Euphrates (1.9-10 ppm), and in the Fatha samples (1.9-34 ppm). Thorium (Th) content in the Anah is (0.04-0.11 ppm), in the unconformity zone (0.07-0.63 ppm), in the Euphrates (0.08-0.25 ppm), in the Fatha (0.09-4.13 ppm). Uranium (U) concentration in the Anah is ranged from 0.23 to 5.54 ppm, in the unconformity zone (0.38-2.65 ppm), in the Euphrates (2.01-12 ppm), and in the Fatha (0.2-2.65 ppm). The values that have been normalized for major elements show significant variation among formations. The Anah Formation (Fig. 7 a) and unconformity zone (Fig. 7 b) has similar values depletion in K_2O, TiO_2, and enrichment in CaO and LOI relative to PAAS. In contrast, the Euphrates Formation (Fig. 7 c) is enrichment in CaO, MgO, and LOI and depletion in K2O, and TiO_2 compared to PAAS, whereas the Fatha Formation (Fig. 7 d) is depleted in Al_2O_3, Fe_2O_3, TiO_2 and enrichment in CaO, MgO, LOI relative to PAAS. These results are, in general, consistent with increased calcite in the formations.

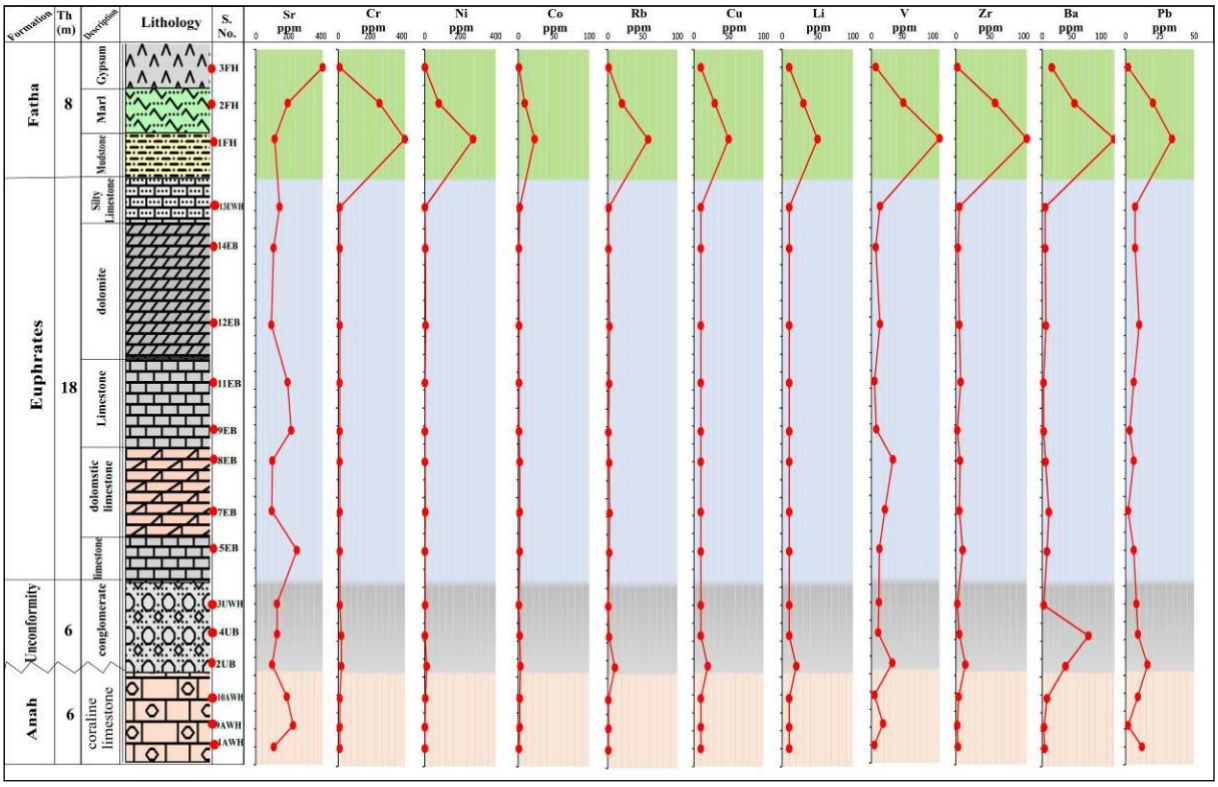

Fig.6. Chemostratigraphic variation in selected trace elements in formations in the study area

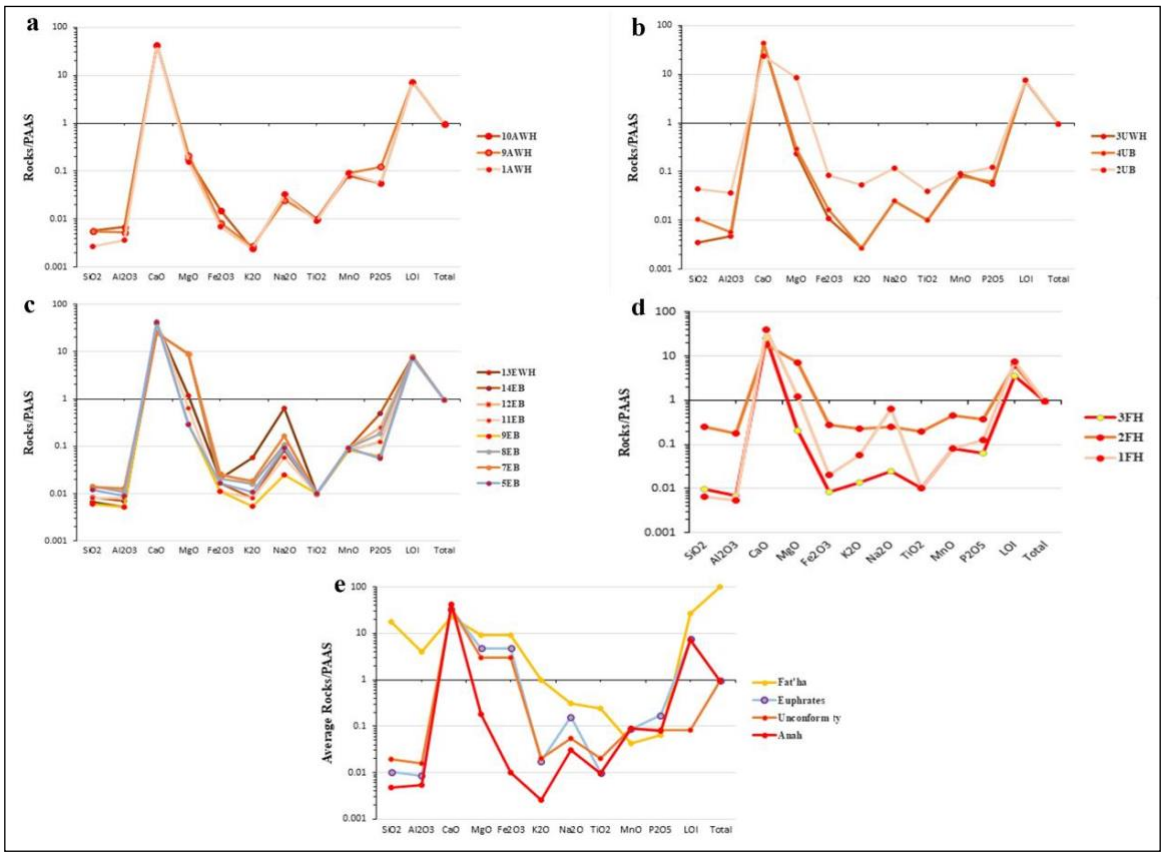

Fig.7. PAAS-normalized major oxides pattern of the Anah Formation (a); Unconformity zone (b); the Euphrates Formation (c); The Fatha Formation (d) and the average of each formation (e)

Data of the trace elements are normalized to PAAS and show considerable variation among formations. The Anah Formation (Fig. 8 a) is enrichment in Zn, Sr, and U relative to PAAS and slight depletion in Ni, Rb, Cs, and Th, while the unconformity zone (Fig. 8 b) is enrichment in Zn compared to PAAS and depletion in Ni, Rb, Cs, Hf, and Th. In contrast, the Euphrates Formation (Fig. 8 c) is enrichment in Zn, Sr, and U relative to PAAS and depleted in Ni, Rb, Ba, and Th. The Fatha Formation (Fig. 8 d) is enriched in Co, Ni, Cu, Sr, and Pb compared to PAAS and depleted in Rb, Ba, and Th.

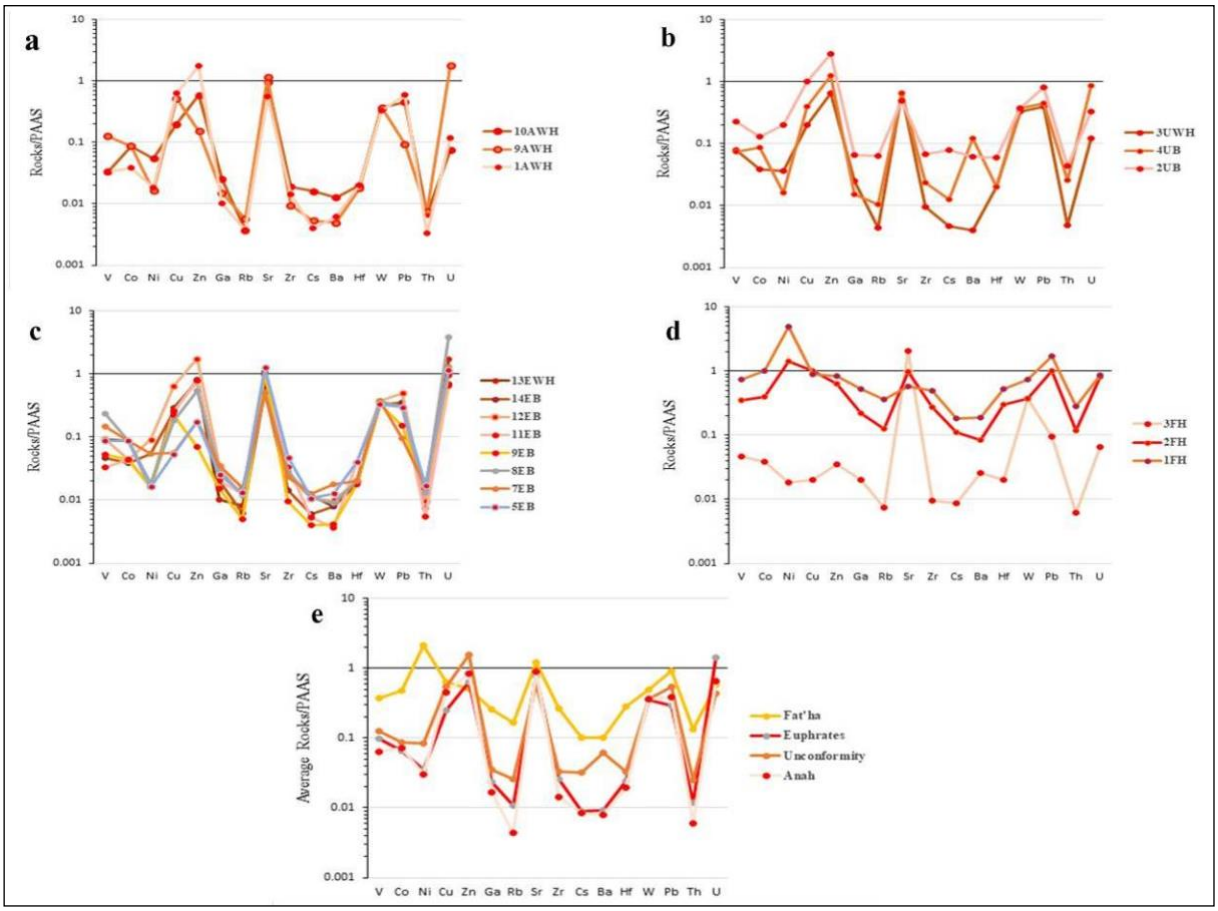

Fig.8.PAAS -normalized trace elements pattern of the Anah Formation (a); Unconformity zone (b); the Euphrates Formation(c); The Fatha Formation(d); and an average of each formation (e).

5. Conclusions

The high contents of CaO, Sr, and a lot of V, and Pb are characteristics of the reef environment as shown in the Anah Formation which was not affected by dolomitization. The unconformity zone is chemically similar to the Anah Formation, with slight differences as it has less content of Sr due to the inversion of aragonite to calcite. The action of weathering, erosion, and leaching redistributes the original elements such as Ba, Rb, Zr, and Li.

The deep environment (Euphrate Formation) is characterized by noticeable variation in Sr, increasing in U, and V and decreasing in Li, Cr, Co, Ni, Cu, Zn, Ga, Rb, Sr, Zr, Cs, Ba, Hf, W, Pb, and Th. The Euphrates Formation has a lot of MgO indicating intensity dolomitization. The lagoonal environment (Fatha Formation) is characterized by a high content of clay minerals, which adsorb high concentrations of Li, V, Cr, Co, Ni, Cu, Zn, Ga, Rb, Sr, Zr, Cs, Ba, Hf, W, Pb, Th, and U. The marl facies contains a moderate content of Ba, Cr, Cs, Hf, Rb, Th, U, V, Sr, Zr, Co, Cu, Li, Ni, Pb, and Zn. In contrast, the gypsum facies showed a sharp decrease in Li, V, Cr, Co, Ni, Cu, Zn, Ga, Rb, Zr, Cs, Ba, Hf, W, Pb, Th, and U and a significant increase in Sr.

Acknowledgements

The authors sincerely thank the Anbar Governorate Office for facilitating fieldwork. The authors are grateful to the Department of Geology, University of Baghdad for providing the facility of the geochemistry labrotary. The authors thank the Iraq Geological Survey for providing permission to use the geological map. The authors thank the laboratory ALS Chemex at Sevilla, Spain, for performing the geochemical analyses.

References

Al-Ankaz, Z.S.A., 2016. Mineralogy and Geochemistry of Bitumen-Bearing Sedimentary Rocks and Sulfur Deposits in Hit – Abu Jir Area, Western Iraq. Ph. D. Thesis (unpublished), University of Baghdad. 158.

Al-Bassam, K. & Saeed, L., 1980. Geochemistry of the carbonate reef and non-reef facies in the Makhmour area, Iraqi Geological Journal, 13(1), 63-83.

Al-Dabbas, M. A., Awadh, S. M., & Zaid, A. A., 2014. Facies analysis and geochemistry of the Euphrates Formation in Central Iraq. Arabian Journal of Geosciences, 7(5), 1799-1810.

Al-Dabbas, M., Awadh, S.M. & Zaid, A.A., 2013. Mineralogy, geochemistry, and reserve estimation of the Euphrates limestone for Portland cement industry at Al-Najaf area, South Iraq. Arabian Journal of Geosciences, 6(2), 491-503.

Al-Obaidy, S.A.H., 2015. Geochemical survey of the Oligocene – Miocene exposures and recent soil between Al - Qaim and Ramadi, West of Iraq. Ph. D. Thesis (unpublished), University of Baghdad, 238.

Al-Sayyab, A. S., & Al-Hamdani, A. T., 1990. Biostratigraphy of the Anah and Euphrates Formations at Wadi Banat Al-Hassan (W. Iraq). Bulletin of the Iraq Natural History Museum, 8(3), 61-83.

Awadh, S.M. & Ahmed, R.M., 2013. Hydrochemistry and pollution probability of selected sites along the Euphrates River, Western Iraq. Arabian Journal of Geosciences, 6 (7), 2501-2518.

Awadh, S.M. & Al-Ankaz, Z.S., 2016. Inorganic geochemistry and origin of bitumen intruded in Euphrates and Fatha Formations in Hit Area, Western Iraq. Iraqi Journal of Science,57(4A), 2478-2489.

Awadh, S.M. & Hussien, S.A., 2015. Organic geochemistry and stable carbon isotopes of oil seepages in the Abu-Jir Fault Zone at Al-Anbar Governorate, Iraq. Iraqi Journal of Science,56(4B), 3162-3175.

Awadh, S.M., 2014. Stable carbon and nitrogen isotopes and elemental composition and origin of organic matter from the Neogene Euphrates, Injana and Dibdibba formations in Iraq: discrimination between marine and terrestrial environments. Geological Quarterly, 58, 729-736.

Bilings, G.K. & Ragland, P.C., 1968. Geochemistry and mineralogy of the recent reef and lagoonal sediments south of Belize (British Honduras). Chemical Geology, 3(2), 135-153.

Chester, R., 1965. Geochemical criteria for differentiating reef from non-reef facies in carbonate rocks. American Association of Petrolum Geologists, 49(3), 258-276.

Dellwig, O., Hinrichs, J., Hild, A., Brumsack, H. J., 2000. Changing sedimentation in tidal flat sediments of the southern North Sea from the Holocene to the present: a geochemical approach. Journal of Sea Research, 44(3-4), 195-208.

Faure, G., 1997. Principles and Applications of Geochemistry. Upper Saddle River, NJ: Prentice Hall.

Fritz, P., & Katz, A., 1972. The sodium distribution of dolomite crystals. Chemical Geology, 10(3), 237-244.

GEOSURV, 2013. Geological Map of Haditha Quadrangle, Sheet NI-38-5. 1:250.000 quaderanles. GEOSURV, Baghdad, Iraq.

Gonneea, M.E. & Paytan, A., 2006. Phase associations of barium in marine sediments. Marine Chemistry, 100(1-2), 124-135.

Jassim, S.Z. & Goff, J.C., 2006.Geology of Iraq. Published by Dolin, Prague and Moravian Museum, Brno, 341.

Jensen, H., Gaw, S., Lehto, N. J., Hassall, L., Robinson, B. H., 2018. The mobility and plant uptake of gallium and indium, two emerging contaminants associated with electronic waste and other sources. Chemosphere, 209, 675-684.

Jones, B. & Manning, D.A., 1994. Comparison of geochemical indices used for the interpretation of palaeoredox conditions in ancient mudstones. Chemical Geology, 111, 111-129.

López-Buendıa, A. M., Bastida, J., Querol, X., Whateley, M. K. G., 1999. Geochemical data as indicators of palaeosalinity in coastal organic-rich sediments. Chemical Geology, 157(3-4), 235-254.

Mohammed, M. H., & Nasser, M. E., 2018. facies analysis and geological modeling of Euphrates Formation in Ajeel Oil Field, Northern Iraq. Iraqi Journal of Science, 2065-2079.

Rankama, K. & Sahama, T.G., 1951. Geochemistry. Soil Science, 71(1), 78.

Scheffler, K., Buehmann, D., Schwark, L., 2006. Analysis of late Palaeozoic glacial to postglacial sedimentary successions in South Africa by geochemical proxies–Response to climate evolution and sedimentary environment. Palaeogeography, Palaeoclimatology, Palaeoecology, 240(1-2), 184-203.

Sissakian, V. K. & Mohammed, B.S., 2007. Stratigraphy. Iraqi Bulletin of Geology and Mining, (1), 51-124.

Taylor, S. R. & McLennan, S.M., 1985. The continental crust: its composition and evolution.

Till, R.,1971. Are there geochemical criteria for differentiating reef and non-reef carbonates? American Association of Petroleum Geologists, 55(3), 523-528.

Tucker, M.E., 1988. Techniques in sedimentology. Blackwell Scientific Publications.

Tucker, M. E., Purser, B. H., & Zenger, D. H. (Eds.)., 2009. Dolomites: A volume in honour of Dolomieu. John Wiley & Sons.

Turekian, K. K., & Wedepohl, K. H. 1961. Distribution of the elements in some major units of the earth's crust. Geological Society of America Bulletin, 72(2), 175-192

Veizer, J., Lemieux, J., Jones, B., Gibling, M. R., Savelle, J., 1977. Sodium: paleosalinity indicator in ancient carbonate rocks. Geology, 5(3), 177-179.